New Methods Characterizing Avalanche Behavior to Determine Powder Flow

François Lavoie,[1] Louis Cartilier,[1] and Roch Thibert[2,3]

Received December 24, 2001; accepted February 12, 2002

Purpose. To characterize the avalanche behavior of different powders and to compare the results of the strange-attractor and novel characterization approaches.

Methods. The following nine different materials were tested: three lactoses, maltodextrin, two microcrystalline celluloses, sodium chloride, sucrose, and glass beads. Morphology, size, and size distribution, true density, bulk and tap density, angle of repose, flow index, and avalanching behavior were quantified for each excipient by scanning electron microscopy, laser time-of-flight analysis, helium pycnometer, graduated cylinder, fixed-height funnel, Flodex (Hanson Research Corp., Chatsworth, California) method, and AeroFlow (TSI, Inc., St. Paul, Minnesota), respectively. Environmental factors were controlled, and the avalanches were studied at various speeds.

Results. The strange-attractor graph obtained at 1 rotation per 120 s showed that it was difficult to appreciate the flowability differences among 3-mm glass beads, lactose 100, and lactose 325. However, plotting the raw data as a relationship of the time between each avalanche and the inverse of speed revealed a characteristic linear slope for each sample. Furthermore, a new flowability index based on the SD calculated from the raw data gave results that were consistent with Carr's index. A cohesive index also can be determined by avalanche behavior, and it reflects the stability of the rapid particular rearrangements of powder.

Conclusion. A novel method of evaluating avalanche measurements makes it possible to better characterize powder flowability and to predict powder behavior under working conditions.

KEY WORDS: powder flow; avalanche behavior; quantitative analysis; novel flow and cohesion indices; Carr's index.

INTRODUCTION

Powder characteristics such as, for example, particle size, morphology, surface area, absolute density, and distribution, modify the flow behavior of powders (1). Environmental factors, including moisture and static electricity, also influence the flow (2). Several methods are currently used to characterize powder flow: bulk and tap density (3); angle of repose; flow through an orifice (4); and Jenike shear cell (5). They give measurable parameters that describe a powder's ability to flow. Using these results, it is possible to predict the flow behavior of the powder under working conditions. However, the prediction depends on the relationship between each partial answer given by the different analyses conducted on the powder, as the individual contributions of the powder's characteristics to movement are less clear. A way of circumventing this problem is to study the powder under dynamic conditions. One of these solutions is the study of avalanches. This dynamic measurement results from the contribution of each parameter and is closer to working conditions. Recently, Iacocca and German (6) proposed to use the AeroFlow because this apparatus allows the powder to flow unconstrained and the resolution of the method is capable of detecting subtle changes in flow behavior. Using a single rotation speed, they plotted histograms of relative frequency vs. time between consecutive cascades and constructed cumulative distributions presenting a log-normal relationship. The slope of the linear portion of the sigmoidal curve obtained is used to measure flowability, with higher values being characteristic of increased flowability.

The avalanche can be divided into three parts: the preavalanche period; the avalanche; and the postavalanche period. Using these divisions, the description of the phenomena is simplified.

The Preavalanche Period

Cohesion forces maintain particulate arrangement inside granular material. These internal cohesion forces can be divided into two categories: extrinsic and intrinsic forces of cohesion (7). Extrinsic forces of cohesion are defined as those that hold particles together, but are not directly connected to the nature of the powder itself and depend on environmental factors. Among the various environmental factors, moisture and static electricity are the most important (8). Moisture influences the powder bed by the formation of a thin water film on the surface of the particles, creating water bridges and stabilizing particulate position (9). Static electricity is a factor that varies in intensity according to the environmental medium and the qualities of the powder. Intrinsic cohesive forces are specific to the characteristics of the powder. Particle size, shape, surface area, and surface roughness influence these forces. Surface area is a key parameter. A smooth surface, in comparison with a rough surface, offers less resistance to movement. Indeed, the forces of friction and adhesion are influenced by the contact surface. Finally, electrostatic forces depend on surface area. Particle morphology and size influence the behavior of powders. Size is also a factor influencing the stability of particulate arrangement of the powder. With a narrow distribution of particle sizes, the powder loses possibilities of rearrangement and is consequently less dense. All these factors account for cohesion forces between particles and act against gravity when an avalanche is about to occur.

Gravity is a force that always acts vertically. It is, however, possible to chart a result of this force acting on the surface of a tilted plane. The vector of the internal force is opposed to this resultant. In a rotating disc containing powder, the angle of inclination of the powder when the two opposite forces are in perfect balance is called a dynamic angle of repose (10). Thus, the dynamic angle of repose represents the balance between internal forces and gravity. Although gravity is constant, cohesion is not because cohesion results from multiple factors. Several combinations of the latter have the possibility of giving the same result.

The Avalanche

An avalanche occurs when the balance between cohesion and gravity is broken. During this second phase, powder char-

[1] Faculté de Pharmacie, Université de Montréal, Montréal, Québec, Canada H3C 3J7.

[2] Pharmaceutical R&D Merck Frosst Canada & Co., 16711 Trans-Canada Highway Kirkland, Quebec, Canada H9H 3L1.

[3] To whom correspondence should be addressed. (e-mail: roch_thibert@merck.com)

0724-8741/02/0600-0887/0 © 2002 Plenum Publishing Corporation

acteristics (i.e., size, morphology, particulate density, and distribution) will act again in different ways, this time providing the dynamics of the system. Two phenomena are present at the time of an avalanche: the distance covered by the particles and the segregation of the surface (11–14). Both tend to provoke different density regions that will influence avalanche behavior. The existing link between these two phenomena is less well-defined.

The Postavalanche (Resting) Period

Following the avalanche, the powder slope changes. The angle formed between the slope and a horizontal plane is known as the static angle of repose. It is smaller than the dynamic angle of repose and is correlated to the quantity of avalanched mass. The avalanche modifies the degree of aeration, which will tend toward an equilibrium after some cycles of avalanches that occur during rotation.

The main objective of the study was to evaluate the avalanche behavior of powders using the AeroFlow instrument. An important aspect of this work is that various drum speeds were tested to obtain a specific series of results for each powder. Considering that the environmental factors influencing avalanches are moisture and static electricity (15), and that the powder-related factors are morphology, size, and density, the experimental protocol accomplished the following: (1) determined the particle morphology, size, and distribution, and the true density for the excipients; (2) controlled the environmental factors; and (3) studied the phenomenon of avalanches at various speeds. The goals of the study were the following: (1) to draw up a standard protocol combining the factors to be controlled; (2) to investigate the avalanche behavior of different powders; (3) to propose new indices characterizing the fluidity and cohesion of the powders; and (4) to compare the new avalanche method with already existing methods known to evaluate the packing rearrangements of particles.

MATERIALS AND METHODS

Materials

Nine different materials were tested: lactose 100 (Pharmatose 100M, lot 022821; DMV International Pharma, Veghel, The Netherlands); lactose 200 (Pharmatose 200M, lot 024801); lactose 325 (Pharmatose 325M, lot 043805); maltodextrin (Maltrin M150, lot M9617236; Grain Processing Corporation, Muscatine, Iowa); microcrystalline celluloses (MCCs) (Avicel PH103, lot 3756 and Avicel PH105, lot 5904; FMC Biopolymer, Philadelphia, Pennsylvania); sodium chloride (American Chemical Ltd., Montreal, Quebec, Canada, lot w-93-47/65670-940107); sucrose (Lantic, Montreal, Quebec, Canada, lot M9195); and glass beads (3-mm diameter; Potters Industries, lot 101097; Valley Forge, Pennsylvania).

Methods

Scanning Electron Microscopy (SEM)

This method served to visualize the morphology and surface aspects of particles at 100× magnification. Each sample was gold-coated with a sputter coater (Auto 306, Edwards, Crawley, West Sussex, England) and observed with a scanning electron microscope (JSM-820, JEOL, Tokyo, Japan).

Particle Size Determination

The Aerosizer (TSI Inc., St. Paul, Minnesota) is a system designed to measure the size of particles. Particle size resolution is 0.2–700 μm. To measure the particle sizes of the powder samples, the shear force, feed rate, and deagglomeration were set to "high" and the pin vibration was set to "on." If the average particle size of the sample was higher than 20 μm, the photo multiplier tube was set to 850 V; otherwise, it was set to 1100 V. Each material was tested three times.

True Density

Results were obtained with a helium pycnometer (Ultrapycnometer 1000, Quantachrome, Boynton Beach, Florida). The samples were stored for 24 h in a vacuum chamber, and measurements were made following standard operating procedures.

Angle of Repose

The angle of repose was determined by using the fixed-height funnel method (i.e., by measuring the cone height vs. the base formed by the powder falling through a plastic funnel placed approximately 5 cm from the table surface until a stable cone was produced). Each material was tested three times.

Powder Flowability Index

The Flodex (Hanson Research Corp., Chatsworth, California) was used to provide an index of powder flowability. The method is based on the ability of a powder to fall freely through a hole in a plate. The results are given as the millimeter diameter of the smallest hole through which the powder falls freely three consecutive times. It represents the size of the hole that overcomes the side friction of the powder core cylinder by its weight. The procedure followed is based on that given in the manufacturer's operation manual.

Bulk and Tapped Density Determination

The bulk and tapped densities were determined according to the method described in the United States Pharmacopeia U.S.P. XXIV, Method ⟨616⟩ Bulk density and tapped density (The United States Pharmacopeia Convention Inc., Rockville, MD, pp. 1913–1914). A 100-ml glass cylinder was weighed, then was filled with 40 ml of powder and reweighed. The open extremity was secured with Parafilm (Pechiney Plastic Packaging, Neenah, Wisconsin). The cylinder was gently reversed and redressed once, and the powder was carefully leveled without compacting. The loose density was determined after one mechanical tap in a tapping machine (J. Engelsman, Ludwigshafen a. Rh., Germany). The bulk density was measured by dividing the mass by the volume. The same measurement was repeated after 2000 taps for tap density. Carr's index was established using Eq. 1:

$$\text{Carr's index} = \frac{100\ (\rho_{bulk} - \rho_{tap})}{\rho_{bulk}} \quad (1)$$

Determination of Powder Avalanches

The AeroFlow uses a transparent disc. A photocell array located behind the disc collects information on the quantity of

light passing through the disc. As the disc rotates, the photocell array records light variations during the cyclic formation of avalanches. The results are expressed as the time between each avalanche, which represents the duration of a complete cycle (i.e., preavalanche, avalanche, and resting periods). An aluminum screen (≈ 40 squares/cm^2) covered the inside perimeter. Powder was trapped in the small squares, and an avalanche was formed against the powders internal forces rather than against the disc wall. The volume of powder used was 40 ml. Prior to each experiment, the powder also was sieved with an 18-mesh sieve and was conditioned for at least 24 h in a humidity-controlled chamber at 30% relative humidity at room temperature. The chamber was made up of saturated MgBr2 salt solutions in a desiccator (16). Each experimental time period was 600 s, and for the new analysis method each powder sample was tested at 25 different speeds that varied between 25 and 240 s per rotation (i.e., 25; 30; 35; 40; 45; 50; 60; 70; 80; 90; 100; 110; 120; 130; 140; 150; 160; 170; 180; 190; 200; 210; 220; 230; and 240 s per rotation).

RESULTS AND DISCUSSION

Using SEM, the goal was to visualize the aspect, shape, and size distribution of the powders. Lactose 200 particles (Fig. 1b) are rounded and less elongated when compared to lactose 100 and lactose 325 particles (Fig. 1, a and c), which show a crystalline and elongated shape. Sucrose crystals are irregularly shaped and present a smooth surface (Fig. 1d). Sodium chloride crystals are almost cubic with a smooth surface (Fig. 1e). Maltodextrin is composed of small rounded

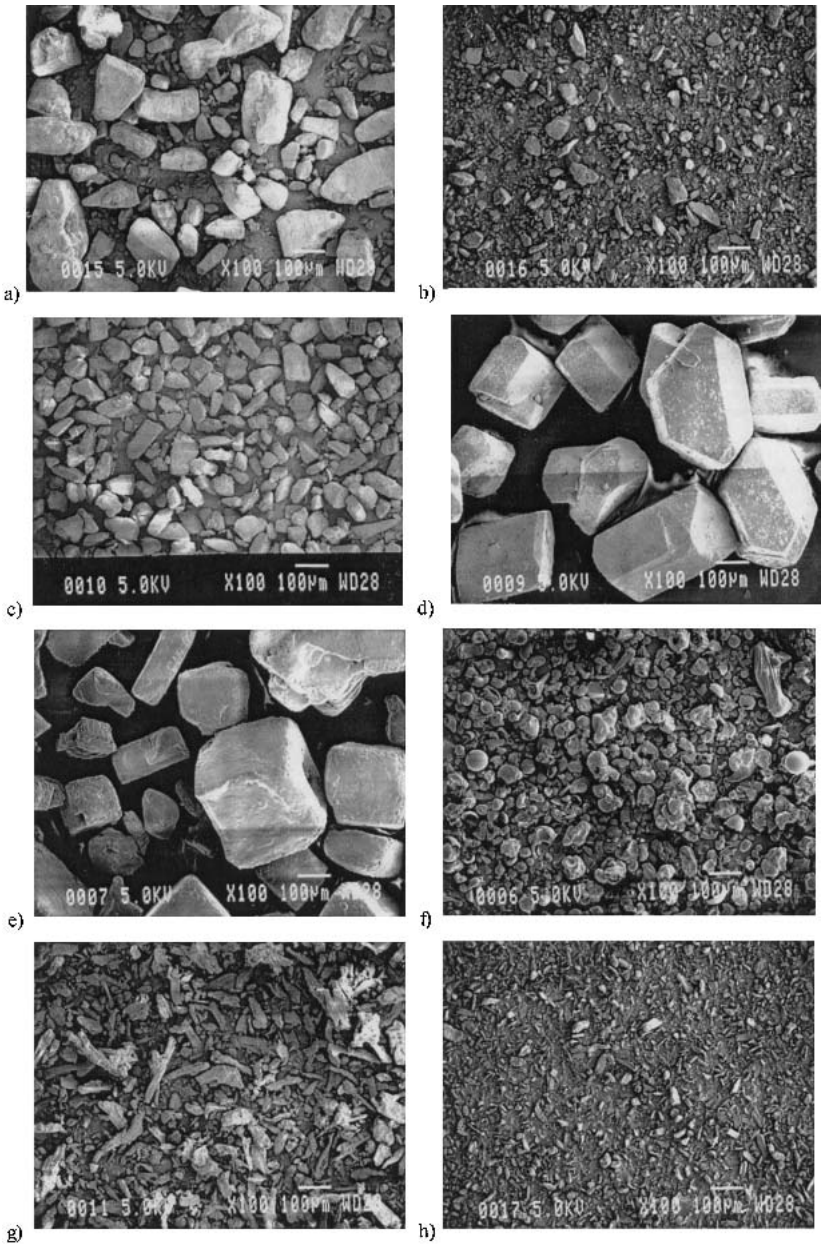

Fig. 1. SEM image (100×) of (a) lactose 100, (b) lactose 200, (c) lactose 325, (d) sucrose, (e) sodium chloride, (f) maltodextrin, (g) MCC 103, and (h) MCC 105.

Table I. The Aerodynamic Particle Size and Size Distribution of Tested Materials[a]

Materials	5% Under	50% Under	95% Under	Span
MCC 105	5.8	14.9	23.8	1.21
MCC 103	11.4	28.0	43.6	1.15
Lactose 200	8.9	28.2	45.6	1.30
Maltodextrin	15.9	44.0	68.9	1.21
Lactose 325	30.7	50.7	69.4	0.76
Lactose 100	37.7	93.6	139.2	1.08
Sodium chloride	115.8	209.7	364.3	1.19
Sucrose	185.9	320.3	524.2	1.06

[a] Values given as μm.

particles, the shape of which has the characteristics of a spray-dried product (Fig. 1f). The MCC products, 103 and 105, have needle-like particles with a rough surface (Fig. 1, g and h).

Particle size measurements were made in triplicate. Table 1 summarizes the particle aerodynamic sizes (5%, 50%, and 95% under) of the tested materials. These results supported the observations from the SEM images. However, lactose 200 had the broadest particle size distribution. Lactose 325 is a sieved product, which explains its very narrow size distribution. The general shapes of the curves for maltodextrin and lactose 100 are similar, but lactose 100 is composed of larger particles. The sodium chloride particle size distribution is broader than that of sucrose, which is almost as narrow as that of lactose 325.

Most of the products had similar true densities of approximately 1.5 g/cm^3 (Table 2). However, maltodextrin, sucrose, and sodium chloride had slightly different true densities of 1.37, 1.58, and 2.16 g/cm^3, respectively.

The results of flowability measurements, as assessed by angle of repose, are presented in Table 2. The method is frequently used because of its ease of determination, but the reproducibility of the measured angle, as well as its range of application, is quite poor. Some powders form more than one angle of repose, and difficulties arise as to which angle is correct (6). Such is case with lactose 200, MCC 105, MCC 103, and maltodextrin (i.e., cohesive powders). Hence, these are the powders that require a precise determination of flowability. On the other hand, glass spheres show some rebound effect that does not allow the formation of any packing assembly. It seems that this method allows two groups to be distinguished: lactose 325 and lactose 100 present a lower flowability than sucrose and sodium chloride. Thus, this method does not mimic the working conditions, and it presents a poor reproducibility, a rather gross power of discrimination, and a limited range of application.

The Flodex results are presented in Table 2. This technique was able to distinguish three groups of behaviors: (1) good flowability (sodium chloride and sucrose); (2) intermediate flowability (lactoses 100 and 325); and (3) low flowability (lactose 200 and MCC 105). However, this kind of information is of little use as we are just able to distinguish large categories of flowability profiles. Again, this type of measurement is far from working conditions and does not represent the powder behavior under dynamic conditions. Hence, a flowing powder could become nonflowing when forced through small openings, depending on factors like particle size and morphology or the presence of lubricants, for example (6).

The powder flow behavior was evaluated with the concept of the strange attractor (17). Kaye (18) has developed a visual technique to express the fluidity of a powder that applies to time series such as the results of experiments on avalanches. The time between each avalanche (i.e,., T1, T2, T3, etc.) is used to create a series of coordinates of points (i.e., T1, T2; T2, T3; T3, T4, etc). These coordinates reveal a scatterplot, called the drawing of attraction. It is centered on a point known as the point of attraction, in the vocabulary of deterministic chaos. The width of the scatterplot expresses the fluidity of the powder. Powder presenting the most centered cloud on its point of attraction has the best fluidity.

A visual analysis of strange-attractor graphs (Fig. 2) that were obtained at one rotation per 120 s for all the tested materials resulted in the following ranking with respect to fluidity:

sucrose > sodium chloride > glass beads> lactose 325 > lactose 100 > MCC 103 >lactose 200 > maltodextrin > MCC 105

The AeroFlow manufacturer recommends this procedure for powder flowability analysis. It is a qualitative method that presents a good distinction between the flowability of sucrose and that of MCC 105. These represent extreme conditions: the best and the worst flowability profiles. Obviously, it is more difficult to distinguish differences among the other powders.

Table II. Selected Physical Properties and Flow Indices of Tested Materials[a]

Materials	True density (g/ml)	Angle of repose (°)	Flodex index (mm)	Carr's index (%)	Cohesion index	Flowability index
Lactose 100	1.53	38 ± 2	17	20	2.87 ± 0.20	1.05 ± 0.07
Lactose 200	1.51	[b]	29	41	6.43 ± 0.02	2.82 ± 0.36
Lactose 325	1.51	41 ± 1	19	23	3.93 ± 0.50	1.17 ± 0.10
MCC 103	1.51	[b]	—	19	7.10 ± 0.04	1.82 ± 0.06
MCC 105	1.51	[b]	>34	22	NA	NA
Maltodextrin	1.37	[b]	—	24	9.83 ± 0.03	3.55 ± 0.01
Sodium chloride	2.16	34 ± 1	5	15	5.18 ± 0.02	0.83 ± 0.03
Sucrose	1.58	35 ± 1	<4	10	3.45 ± 0.15	0.18 ± 0.02
Glass beads	2.47	NA	—	4	2.73 ± 0.13	1.09 ± 0.22

[a] Values given as mean ± SD, unless otherwise indicated. NA, not applicable.
[b] Powder presents more than one angle of repose.

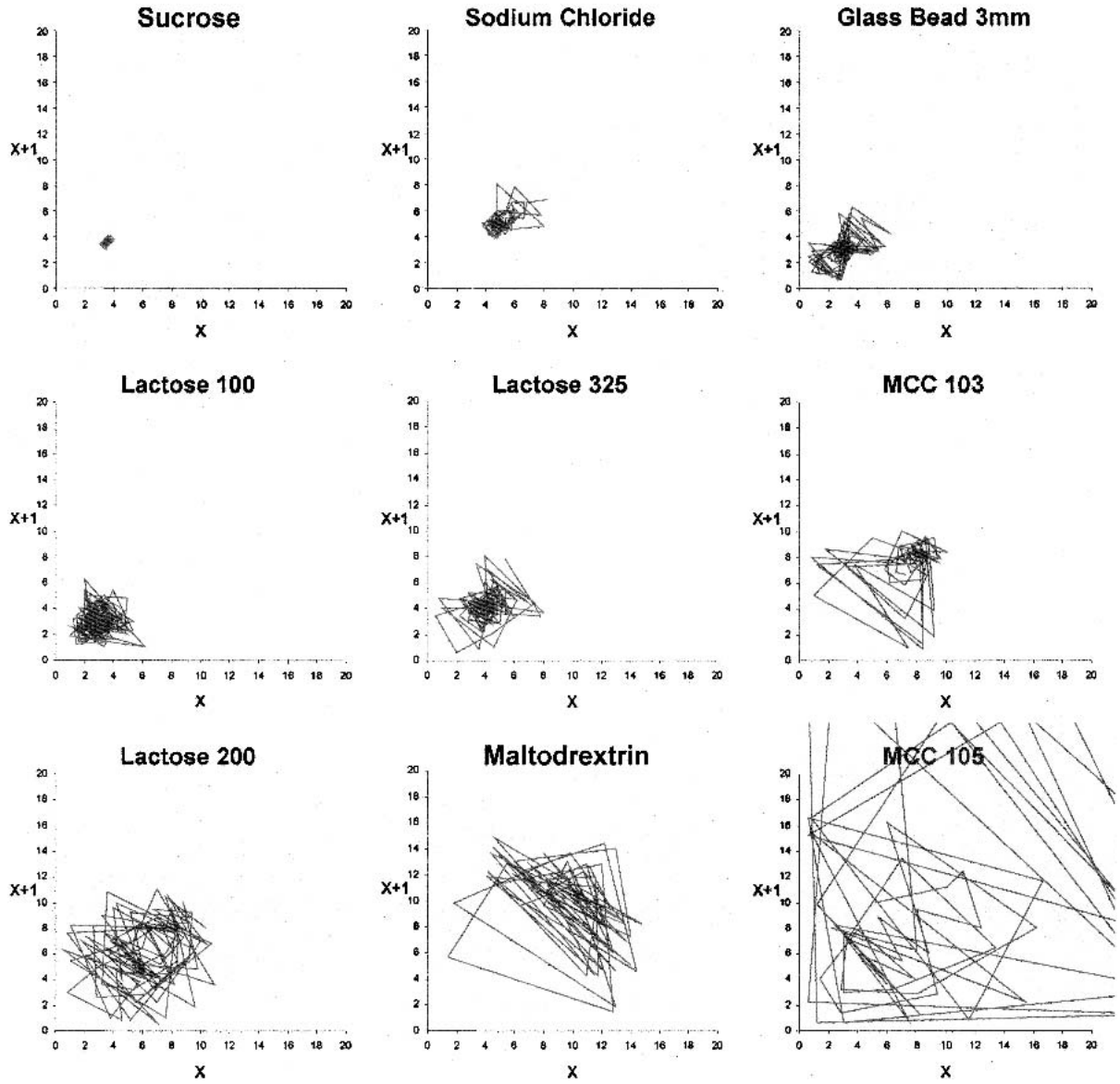

Fig. 2. The strange-attractor graphs for materials tested at one rotation per 120 s.

This led to a novel approach with which to evaluate the avalanche method, whereby the expression of the time series results (time (seconds)/avalanche) as a function of inverse speed (1/speed) revealed a linear relationship between these two parameters (Fig. 3). A different slope for each powder can be distinguished. Each slope represents the combined influence of size, size distribution, density, morphology, and chemical nature. Some lines cut across each other, and some of them share a similar value for the same speed. Using a range of speed to calculate a single index allows each powder to be distinguished quantitatively, contrary to previous approaches using a single rotation speed (6). The MCC 105 value was rejected because the experimental setting was not efficient in preventing its solid-like behavior at all rotational speeds.

To quantify or measure the flow behavior, a new granular index of fluidity was proposed. At each rotation speed, there is an average avalanche time with an SD. This SD gives

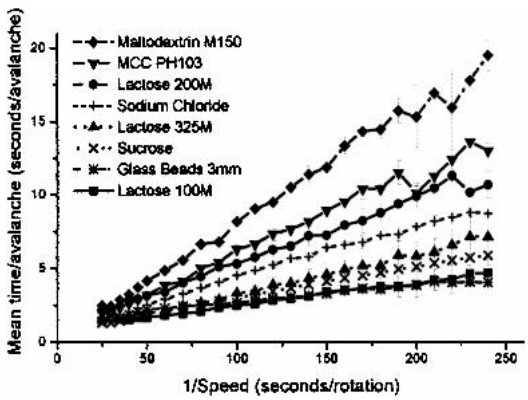

Fig. 3. Mean time to avalanche results as a function of inverse speed.

the dispersion of the results around the average. Significant deviations from the average result from poor fluidity or the unstable character of a powder; a low deviation is a sign of great fluidity. This SD, established for a given speed, runs up against the problems of sensitivity; the probability of obtaining the same result for two powders that behave differently is real (see, for example, the case of lactose 200 and MCC 103). For this reason, the index of fluidity is determined by the average of SDs obtained for various speeds to decrease the risk of false identical results. The SD is thus determined for various speeds, from the first to the *n*th speed tested. The formula of the flowability index is shown below:

$$\text{Flowability index} = \frac{1}{n}\sum_{i=1}^{n} Si \tag{2}$$

where n represents the total number of speeds tested in the experiment (in this case, n = 25), and Si represents the SD of the tested speed. According to the flowability index (Table 2), the rank of the tested powders should be:

sucrose > sodium chloride > lactose 100 = glass beads > lactose 325 > MCC 103 = lactose 200 > maltodextrin

It is also interesting to link these values to a well-established method (i.e., Carr's index) (Table 2). Comparisons between Carr's index and the flowability index have shown a direct relationship for five of the tested materials (lactose 100, lactose 200, lactose 325, sucrose, and sodium chloride) (Fig. 4, lozenges). This can be explained by the regular shape and cube-like morphology of their particles that influence the flowability by their packing formation. For the other samples, (MCC 103, maltodextrin, and glass beads), Carr's index may not represent the most appropriate parameter with which to characterize the flow behavior due to its inability to account for particle morphology (Fig. 4, squares). In the case of MCC 103, the needle-like morphology of the particles causes entanglements that absorb the stress caused by the tapping machine and interferes with the creation of a denser powder conformation. This results in a lower Carr's index value that does not reflect the real flow behavior of the powder. In the case of glass beads and maltodextrin, the situation is completely different. The low Carr's index value is caused by the efficiency of the natural packing formation of sphere-like morphology. The flowability index, established by powder movement measurement, has shown that it is possible to characterize and differentiate the kinetic behavior of a powder that has not been properly evaluated by Carr's index. Indeed, the slow particulate rearrangement obtained with Carr's index (i.e., the tapping cylinder method) does not properly evaluate the normal behavior of some peculiar powders under working conditions.

In addition to the new flowability index, a new granular index of cohesion also was proposed. The time elapsed between two avalanches is an expression of the capacity of the powder to absorb stress. It reflects the difference between the static and dynamic angles of repose. Typical raw data for MCC 103 at 240 s per rotation are shown in Fig. 5. For time t_i, which was defined as the time at which an avalanche occurs and is described as (t_1; t_2; …; t_i; t_m), and m, which is the total number of avalanches of the series, the average time between two events can be calculated using Eq. 3:

$$\bar{x} = \frac{1}{m}\sum_{i=1}^{m-1} t_{(i\times 1)} - t_i \tag{3}$$

To make the procedure more robust and to avoid false identical values, the index of cohesion is based on the average of average times between two avalanches for the different speeds selected. For (x_1; x_2; …; x_j; x_n), the cohesion index is calculated using Eq. 4:

$$\text{Cohesion index} = \frac{1}{n}\sum_{j=1}^{n} \bar{x}_j \tag{4}$$

where n represents the total number of test speeds. When n is fixed, the integer j varies from 1 to n.

It should be noted that this cohesion index, as well as the flowability index, depends on the range and selection of the speeds tested, and that these experimental conditions should always be mentioned in the method description when comparing various data (Table 2). Thus, the cohesion index re-

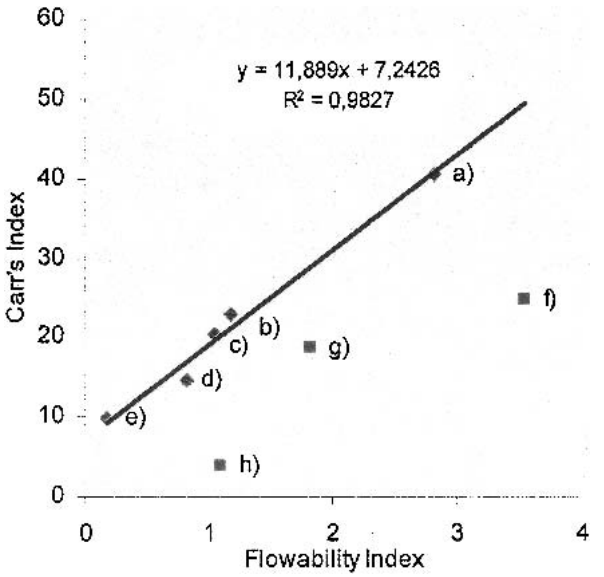

Fig. 4. Comparison between Carr's index and the new flowability index. A, lactose 200; b, lactose 325; c, lactose 100; d, sodium chloride; e, sucrose; f, maltodextrin; g, MCC 103; and h, glass beads.

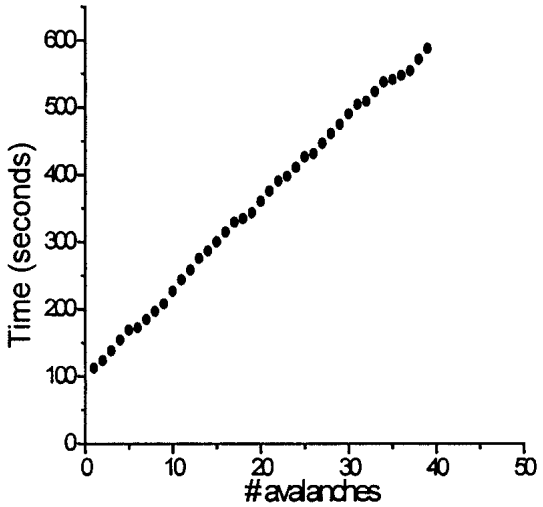

Fig. 5. Raw data of MCC 103 at 240 s per rotation after removing the first 100 s.

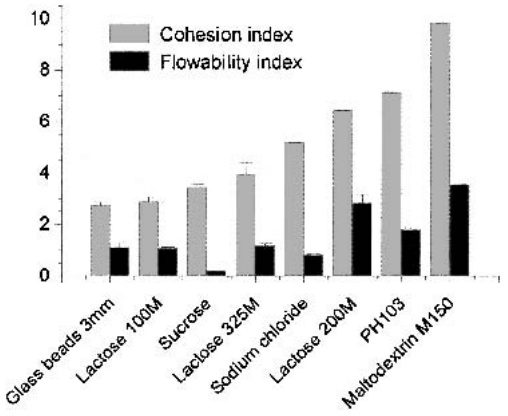

Fig. 6. New cohesion index as a function of the new flowability index.

flects the inertia of the powder vis-à-vis movement. The larger this value will be, the more the powder will tend to behave like an agglomerated mass of particles. Many factors influence the cohesion index, but the most important seems to be the morphology of the powder particles. For example, sucrose has a cohesion index lower than that of sodium chloride. Particle conformation could explain these results. Sodium chloride with its cube-like morphology should create much more stable packing compared to sucrose with its rhombohedral-like particles. For glass beads, the failure lines created by their spherical conformation are reflected by the cohesion index value. Cohesion and flowability indices are obtained with the same group of data. Figure 6 shows that these two indices are independent. The values of the fluidity and cohesion indices are reproducible under the same experimental conditions. Although a change in experimental conditions could lead to different results, it is unlikely that a difference will be noticed in the relative appreciation of powder fluidity, even under other working conditions.

CONCLUSION

By standardizing parameters such as moisture and static electricity, the study of powder avalanches was able to differentiate the flow behaviors of various pharmaceutical excipients. Using the new avalanche behavior characterization method, it is possible to obtain, with one set of experiments, two new quantitative indices: fluidity and cohesion indices. Both indices have shown that it is possible to measure dynamic short-term particle rearrangement. The flowability index illustrates a "resistance" characteristic of a powder to initiate movement during an avalanche. It can properly evaluate the flow of different types of powders and granulates. It is important to note the existing relationship between the new flowability index and Carr's index, which measures particle rearrangement phenomena. The cohesion index provides information on the capacity of the powder to be agglomerated. It reflects particle arrangement stability and expresses the vector of the internal forces. That could help in the selection of the mixer's operating principle (e.g., tumbling and high shear). This new approach in powder behavior characterization is promising. Studying the results with the strange-attractor method seems quite interesting. However, the result can be appreciated only in a qualitative manner. Further analysis with the fractal dimension method will be needed to quantitatively evaluate strange-attractor graph.

REFERENCES

1. J. Schweder and D. Shulze. Measurement of flow properties of bulk solids. *Powder Technol.* **61**:59–68 (1990).
2. G. E. Amidon and M. E. Houghton. Powder flow testing in preformulation and formulation development. *Pharm. Manuf.* **July**: 21–31 (1985).
3. A. C. Abdillah and D. Geldart. The use of bulk density measurement as flowability indicators. *Powder Technol.* **102**:151–165 (1999).
4. G. K. Bolhuis and Z. T. Chowhan. Materials for direct compaction. In G. Alderborn and C. Nyström (eds.), *Pharmaceutical Powder Compaction Technology*, Marcel Dekker, New York, 1996 pp. 419–500.
5. Y. S. Lee, R. Poynter, F. Podczeck, and M. Newton. Development of a dual approach to assess powder flow from avalanching behavior. *AAPS PharmSciTech* **1**: Article 21, (2000) http://www.pharmscitech.com.
6. R. G. Iacocca and R. M. German. The experimental evaluation of die compaction lubricants using deterministic chaos theory. *Powder Technol* **102**:253–265 (1999).
7. S. Rastogi and G. E. Klinzing. Characterizing the rheology of powders by studying dynamic avalanching of the powder. *Part. Part. Syst. Charact.* **11**:453–456 (1994).
8. N. Standish. A. B. Yu, and Q. L. He. An experimental study of the packing of a coal heap. *Powder Technol.* **68**:187–193 (1991).
9. L. Bocquet, E. Charlaix, S. Ciliberto, and J. Crassous. Moisture-induced ageing in granular media and the kinetics of capillary condensation. *Nature* **396**:735–737 (1998).
10. J. J. McCarthy, T. Shinbrot, G. Metcalfe, J. E. Wolf, and J. M. Ottino. Mixing of granular materials in slowly rotated containers. *AIChE J.* **42**:3351–3363 (1996) http//www.aiche.org/aichejournal.
11. J. A. Drahun and J. Bridgwater. The mechanisms of free surface segregation. *Powder Technol.* **36**:39–53 (1983).
12. H. A. Makse, S. Havlin, P. R. King, and H. E. Stanley. Spontaneous stratification in granular mixtures. *Nature* **386**:379–382 (1997).
13. J. Baxter, U. Tüzün, D. Heyes, I. Hayati, and P. Fredlund. Stratification in poured granular heaps. *Nature* **391**:136 (1998).
14. J. P. Koeppe, M. Enz, and J. Kakalios. Phase diagram for avalanche stratification of granular media. *Phys. Rev.* **58**:R4104–R4107 (1998).
15. B. H. Kaye, J. Gratton-Liimatainen, and J. Lloyd. The effect of flow agents on the rheology of a plastic powder. *Part. Part. Syst. Charact.* **12**:194–197 (1995).
16. H. Nyqvist. Saturated salt solutions for maintaining specified relative humidity. *Int. J. Pharm. Technol. Prod. Manuf.* **4**:47–48 (1983).
17. B. H. Kaye. Characterizing the flow of metal and ceramic powders using the concepts of fractal geometry and chaos theory to interpret the avalanching behavior of a powder. In T. P. Battle and H. Henein (eds.), *Processing and Handling of Powders and Dusts*, Minerals Metals & Materials Society, Warrendale, PA, 1997 pp. 277–282.
18. B. H. Kaye. Characterizing the flowability of a powder using the concepts of fractal geometry and chaos theory. *Part. Part. Syst. Charact.* **14**:53–66 (1997).